


## Biofilm growth on laser-induced periodic surface structures (LIPSS) of AISI 316L stainless steel

Aline Gonçalves Capella<sup>1</sup> , Melquesedeque Moura da Silva<sup>1</sup>, José Guilherme Alvarenga Batista Simões<sup>2</sup>, Vítor Martins de Andrade<sup>3</sup>, Rudimar Riva<sup>1,2</sup>, Katia da Conceição<sup>3</sup>

<sup>1</sup>Universidade Federal de São Paulo, Laboratório de Processamento de Materiais com Laser. Rua Talim 330, São José dos Campos, SP, Brasil.

<sup>2</sup>Instituto de Estudos Avançados, Departamento de Ciência e Tecnologia Aeroespacial. Trevo Cel. Aviador José A.A.do Amarante 1, São José dos Campos, SP, Brasil.

<sup>3</sup>Universidade Federal de São Paulo, Laboratório de Bioquímica de Peptídeos. Rua Talim 330, São José dos Campos, SP, Brasil.

e-mail: aline.capella@unifesp.br, melksilva3000@gmail.com, gmsimoes@gmail.com, vitor.andrade@unifesp.br, rudiriva@gmail.com, katia.conceicao@unifesp.br

### ABSTRACT

The morphological characteristics of metallic surfaces play a crucial role in the adhesion, retention, and growth of bacteria and fungi. Laser-induced periodic surface structures (LIPSS) present potential to controlling biofilm formation on biocompatible metallic surfaces for biomedical and engineering applications. LIPSS have emerged as a promising technique for controlling biofilm formation on biocompatible metallic surfaces in various biomedical and engineering applications. This present work uniquely focuses on investigating the effects of LIPSS on AISI 316L stainless steel (AISI 316L SS) as a potential inhibitor against the adhesion of bacteria and fungi (*E. coli* and *C. albicans*, respectively) on laser-textured surfaces. Microstructural characterization through scanning electron microscopy (SEM), energy-dispersive X-ray spectroscopy (EDX), roughness profiling, and X-ray diffraction (XRD) revealed morphologic alterations of the laser-treated surfaces, resulting in the formation of LIPSS with laser fluences of 2.1 J/cm<sup>2</sup> and 2.8 J/cm<sup>2</sup>, line spacing approximately equivalent to the laser wavelength (532 nm), and average roughness values of 96 nm and 209 nm, respectively. The study found that LIPSS exhibited inhibitory effects against *E. coli* biofilm formation on laser-textured surfaces, with a noticeable enhancement in antimicrobial efficiency ranging from 30% to 43% compared to untreated surfaces. However, the antimicrobial effectiveness against *C. albicans* was notably lower, with marginal improvements observed under specific conditions. Thus, the results showed a complex interplay between surface morphology, microbial adhesion, and antimicrobial efficacy on laser-textured metallic surfaces. These findings underscore the dependence of the antimicrobial properties of laser-textured surfaces on the type of microorganism and laser processing parameters.

**Keywords:** LIPSS; AISI 316L SS; *E. coli* biofilm; *C. albicans* biofilm; Laser-textured surface.

### 1. INTRODUCTION

AISI 316L SS is a biocompatible material used in the production of medical devices, surgical components, and temporary orthopedic implants [1–3]. It is highly employed due to its exceptional corrosion and fatigue resistance, high mechanical strength, good ductility, and biocompatibility. Moreover, its sterilization capability makes it suitable for surgical instruments [4]. However, a critical consideration for using stainless steel in medical component fabrication is the need for its surface to be functional, minimizing bacterial attachment and retention, reducing contamination, cleaning requirements, and corrosion of the component [5, 6].

Well-known pathogens, such as Gram-positive bacteria (e.g., *Staphylococcus aureus*) and Gram-negative bacteria (e.g., *Escherichia coli*), along with opportunistic fungi like *Candida albicans* can colonize and form biofilms on biomedical devices, contributing to product contamination [7–9]. Biofilms consist of populations of microorganisms that adhere to solid surfaces or each other, encased within a self-produced matrix of extracellular polymers (EPS) [10, 11]. They can develop on virtually any natural or manufactured surface, serving as a host that provides a favorable environment for the growth of anaerobic bacteria, other fungal species, and coexisting bacteria [12]. Biofilms exhibit enhanced resistance to antibiotics and other biological or therapeutic related

eradication methods. Their formation and growth on medical devices, like urinary catheters and respirators, can lead to the development of chronic infections, which become resistant and can significantly impact healthcare costs [13]. UK industry estimates that the biofilms can represent a cost of the billions of pounds each year due to product contamination and equipment damage [14].

An alternative approach to inhibit biofilm formation and adhesion to solid surfaces involves modifying the surface topography, roughness, chemical composition, and hydrophobicity. Various manufacturing methods, such as plasma etching, anodic oxidation, chemical vapor deposition, lithography, and electrospinning, have been suggested to achieve antibacterial properties by altering wettability and surface topography [15]. Technologies related to the direct impregnation or coating of the material surface with antimicrobial substances (copper, silver, nitrides, ceramics, organic and inorganic compounds) and/or surface modification through micro- or nano-texturing have demonstrated microbial activity inhibition, influencing biofilm adhesion and growth on these surfaces [16, 17].

The literature has reported several studies on the influence of morphologic alterations on bacterial adhesion to solid surfaces. It has been shown that morphological features of different length scales ranging from nano- to micrometer have strong influences on cell adhesion. In general, materials that are rougher and high hydrophobic tend to promote the development of biofilms more rapidly [18, 19]. However, the literature also has been reported that electropolished stainless steel surfaces could be potential areas for the bacteria colonization [20]. It is important to note that the attachment of microorganisms on the surfaces remains a complex phenomenon that is not fully understood. Studies have shown that surface roughness greater than 0.8  $\mu\text{m}$  is more susceptible to the adhesion and growth of microorganisms [21] due to a higher surface area for attachment, and it is also more challenging to clean [22]. Bacterial adhesion to stainless steel was compared between smooth and rough surfaces in investigations conducted by WHITEHEAD *et al.* [23] and BOYD *et al.* [24]. The authors demonstrated that a surface average roughness on the order of tens of micrometers, similar in scale to the diameter of *S. aureus* cells, promoted strongest attachment to the substrate.

Nanostructured morphological changes have demonstrated the potential to prevent and inhibit the growth of biofilms. Morphological nanostructures can assume various forms, including roughness, relief patterns, nanopillars, and surface nanostructures. The literature has explored the impact of nanoscale morphologic surfaces on microorganism adhesion [25, 26]. NGUYEN *et al.* [27] conducted a comprehensive study on the significance of topography sizes and their effects on cell adhesion, morphology, alignment, and neurite guidance. The authors provided extensive results regarding the influence of sizes on neurite guidance.

Laser texturing is an alternative technology for modifying micro or nanostructured surfaces with dimensional accuracy, reproducibility, and high processing speed [28, 29]. It is possible to create metallic surfaces with nanostructured topographies, a technique known as Laser-Induced Periodic Surface Structures (LIPSS) [30]. The LIPSS can promote chemical changes of the surface, especially when the material processing is performed under active atmosphere [31]. The spacing of the LIPSS structures generated by ultrashort pulsed lasers (femtosecond or picosecond pulses) is generally smaller than half of the laser irradiation wavelength, while LIPSS produced by long-pulsed lasers (> nanosecond pulses) typically have structures spaced at the order of the laser wavelength [32]. Furthermore, the use of fs or ps pulsed lasers results in a smaller heat-affected zone (HAZ) in the material compared to that obtained with ns pulsed lasers, although the processing time with ultrashort pulses is longer due to their lower average power. So, the most studies about the LIPSS on the metallic surface is related to the employment of the femtosecond lasers that have shown the influence of the structures on the surface wettability, beside the transition from the hydrophilic to the hydrophobic state of the textured material [31–34], being the LIPSS performed by nanosecond lasers less explored.

The characteristics of the topography and hydrophobic surface in relation to bacterial/fungal retention have been the subject of extensive research [35–37]. A study conducted by LUTEY *et al.* [35] evaluated the relationship between bacterial cell geometry and the antiadhesion effect on the surface by comparing bacterial retention on different morphological surfaces. The results showed that mirror-polished surfaces favored *E. coli* adhesion, while *S. aureus* retention was inhibited under the same conditions. Furthermore, Laser-Induced Periodic Surface Structures (LIPSS) reduced *E. coli* and *S. aureus* adhesion by approximately 99.8% and 84.7%, respectively. The response of *C. albicans* biofilm production was also examined on both control (flat glass coverslip) and nanostructured surfaces. The results indicated that the fungal cell response was influenced by the nanostructured surfaces, leading to a reduction of the quantity and growth of *C. albicans*. On the other hand, the authors suggested that in medically relevant environments where fungal and bacterial microbes coexist, the biological response to the properties of nanostructured surfaces may be more complex [36]. EPPERLEIN *et al.* [37] assessed the behavior of microbial adhesion to Laser-Induced Periodic Surface Structures (LIPSS) using laser fluences close to the ablation threshold while scanning the sample in a multi-pulse regime. The results

showed that *E. coli* preferentially avoided adhesion to the LIPSS-covered areas, whereas *S. aureus* favored these areas for colonization.

The focus of the current study was to evaluate Laser-Induced Periodic Surface Structures (LIPSS) on AISI 316L SS samples, generated with a simple, fast, and cost-effective nanosecond pulsed laser, as potential inhibitors of microorganism adhesion on laser-textured surfaces when compared to untextured specimens. *Escherichia coli* (*E. coli*) bacteria and *Candida albicans* (*C. albicans*) fungi were considered to quantify the performance of the textured surface. Notably, it is worth emphasizing that LIPSS, typically associated with faster pulse durations (femtoseconds or picoseconds), are being examined here within the context of nanosecond laser pulses.

## 2. MATERIALS AND METHODS

### 2.1. Material

Cylindrical disks of AISI 316L stainless steel with 3 mm diameter and 10 mm length were used as base material. Sample surfaces were previously submitted to usual metallographic preparation, being polished to a mirror-like finish, and cleaned before their processing in ultra-sound bath with acetone for 10 min. To validate its elementary chemical composition, the polished surfaces were characterized by scanning electron microscopy (SEM, Inspect S50, with EDS, EDAX).

### 2.2. LIPSS setup

A linearly polarized beam of a 532 nm Nd:YAG laser (Coherent, Corona), 70 W maximum average power, 100 ns pulse duration, and 5 kHz repetition rate ( $f$ ) was used to generate LIPSS on the upper face of the cylindrical disk. The laser beam scanning on the sample surfaces was performed by a scanning device (SCANLAB, HurrySCAN20) focused with a 250 mm focal length F-Theta objective lens on the AISI 316L SS surface. LIPSS was performed on metallic surface under atmosphere ambient with bidirectional movement of the laser beam, considering scanning speed ( $v$ ), 50 mm<sup>2</sup>, pulse overlapping of 92%, and 600  $\mu$ m spot diameter ( $2w$ ). The parameters are summarized Table 1 and were considered based on previous results [38].

The roughness evaluation of the surfaces was determined through a calibrated profilometer (Taylor-Hobson PGI 1000), by direct contact, after its texturing. Surface roughness was measured using a transverse speed of 0.5 mm/s with a diamond-tipped stylus running, in an area of 1 mm  $\times$  1 mm to obtain the Sa (arithmetical mean height), Sz (maximum height) and Sq (root mean square height) parameters. The microstructure of the textured surfaces was analyzed by scanning electron microscopy (SEM, FEI Inspect S50) and energy-dispersive X-ray spectroscopy (EDX). X-ray power diffraction (XRD Rigaku, Ultima IV), equipped with a Bragg Brentano diffractometer and Cu-K $\alpha$  radiation (wavelength: 0.154056 nm), was conducted to characterize the microstructure of AISI 316L surface, considering beam scanning between 30° and 100° ( $2\theta$ ), angular velocity of 10°/min and step of 0.2°. The obtained diffractograms were analyzed by comparison to the patterns present in the High Score software library.

### 2.3. Bacterial and fungi adhesion on the surface

To evaluate biofilm growth on laser textured surfaces, experimental proceedings were conducted based in previous protocol [39]. The bacteria *Escherichia coli* (*E. coli*), and the fungus *Candida albicans* (*C. albicans*) stored in glycerol stocks at 20%v/v and -80% were used. The microorganisms were previously grown in selective medium Brain heart infusion broth (BHI) and cultured for 24 hours at 36° C. Control (polished surface) and laser textured samples were sterilized for 24 h in 70% alcohol and autoclaved at 120° C for 20 min. Then, for biofilm adherence, the samples were placed onto a 48 wells microplate with 2000  $\mu$ L of standardized suspensions of *E. coli* and *C. albicans* (103 cells/mL) and incubated at 37 °C for 24 h. A well with culture medium and a well

**Table 1:** Processing parameters used to LIPSS on AISI 316L SS surface.

NOMENCLATURE	AVERAGE POWER [W]	PULSE ENERGY ( $P_E$ )* [J]	FLUENCE ( $F$ )** [J/cm <sup>2</sup> ]
S2.1	15	3	2.1
S2.8	20	4	2.8

\* $P_E = P/f$ , \*\* $F = 2P_E/\pi(w)^2$ .

with the fungi inoculum were used as controls. After biofilm adhesion, the samples were processed for biomass and CFU counting and for biofilm fixation.

For biofilm biomass quantification, the samples were submitted to evaluation by the crystal violet method, which was based on PETRACHI *et al.* [40] with modifications. Approximately 2000  $\mu\text{L}$  of 0.1% crystal violet dye was added to cover the metal surface, followed by incubation for 15 min. Then, the microorganisms deposited in the samples were eluted by adding 2000  $\mu\text{L}$  of 30% acetic acid for 15 min. Absorbance readings were performed by spectrophotometry at wavelength of 590 nm (Synergy H1, BIOTEK, USA). The biomass was assigned as antibiofilm efficiency and calculated according to Equation 1:

$$\text{antibiofilm efficiency (\%)} = \left( N_c - \frac{N_s}{N_c} \right) * 100 \quad (1)$$

where  $N_c$  represents the number of colonies on the control samples; and  $N_s$  represents the number of colonies on the tested samples.

After 24 hours of biofilm incubation all the liquid content of the well was removed and the AISI 316L SS samples were fixed with methanol and dehydrated with a sequence of washes with ethanol (10, 25, 50, 75 and 100%). To evaluate the biofilm morphology grown on the laser-treated surfaces, these regions were characterized by SEM (FEI, Inspect S50) and SEM-FEG (Tescan, VEGA 3). These regions were previously metalized with a gold film (Quantum, model Q150R E), considering deposition for 90 s at 20 mA.

### 3. RESULTS AND DISCUSSION

#### 3.1. LIPSS of AISI 316L stainless steel

To validate the elementary chemical composition of the AISI 316L SS, EDX analysis was performed (Figure 1). The main alloy elements: nickel (Ni), chromium (Cr) and molybdenum (Mo) are present in the ferrous matrix of the steel, along with a lower quantity of other elements (Figure 1a). The EDX analyzes of the textured metallic surfaces do not show a significant change in chemical composition, when compared to untreated material, including the oxygen concentration, after the material processing for both conditions – lower and higher fluences at 2.1  $\text{J}/\text{cm}^2$  and 2.8  $\text{J}/\text{cm}^2$ , Figure 1b and 1c, respectively. However, previous work of LIPSS formation using nanosecond pulsed laser with similar fluence values employed in preset work, reported by SIMÕES *et al.* [38], showed some level of oxidation on the surface, that influence of the absorption of laser energy. Qualitative analysis for phase identification present in the material was conducted on the untreated and laser-textured AISI 316L surfaces by X-ray diffractometry, as shown in Figure 2. The austenite phase ( $\gamma\text{-Fe}$ ), characteristic of this stainless steel [41], is observed. Additionally, the martensite phase ( $\alpha'\text{-Fe}$ ) was identified in all conditions. This behavior could be associated with phase transformations occurring during the material processing steps, such as lamination and drawing [41]. Finally, the results do not show spectra associated with oxides after laser texturing of the surface, as obtained by EDX analysis. It is highlighted that, although the characterization techniques did not evidence the oxides after laser-texturing surfaces, their resolution is order of micrometer range, while the oxidation of the surface occurs more superficially.

The topography of untreated (polished surface, base material) and textured AISI 316L SS surfaces, processed at 2.1  $\text{J}/\text{cm}^2$  and 2.8  $\text{J}/\text{cm}^2$ , was characterized using profilometry. In Figure 3, the three-dimensional profile of the surfaces is presented. An increase in the roughness is observed for the textured surface processed at higher fluence (Figure 3b) compared to lower fluence (Figure 3c) used to generate LIPSS. The  $S_a$  parameter, representing the difference in height of each point compared to the arithmetical mean of the surface, exhibits an average variation up to two times higher with the increase in laser fluence applied to the surface, resulting in a roughness change from 96 nm to 209 nm after the texturing of the metallic surface. It is worth noting that the average roughness remains low, within in nanometric scale. The literature [42] has demonstrated the influence of surface morphology on the metabolic properties of cells. BRAEM *et al.* [43] highlighted the impact of metallic surface roughness on microbial adhesion and its growth. The results indicate that an average surface roughness between 5–8  $\mu\text{m}$  promotes the *Staphylococcus* bacterial biofilm adhesion compared to surfaces with a roughness value of about 30 nm. Concerning the topography of the untreated surface (Figure 3a), as expected, it was observed some increase in the roughness for textured surfaces, particularly for the material surface processed to higher laser fluence (Figure 3c), when compared to roughness obtained of the polished surface.

Figure 4 presents the SEM of the homogeneous the LIPSS generated on the metal surfaces. It is observed that for both experimental conditions, 2.1  $\text{J}/\text{cm}^2$  (Figure 4a) and 2.8  $\text{J}/\text{cm}^2$  (Figure 4b), there is the formation of periodic nanostructures (red circle, Figure 4a), characteristic of LIPSS, evidencing the efficiency of nanosecond

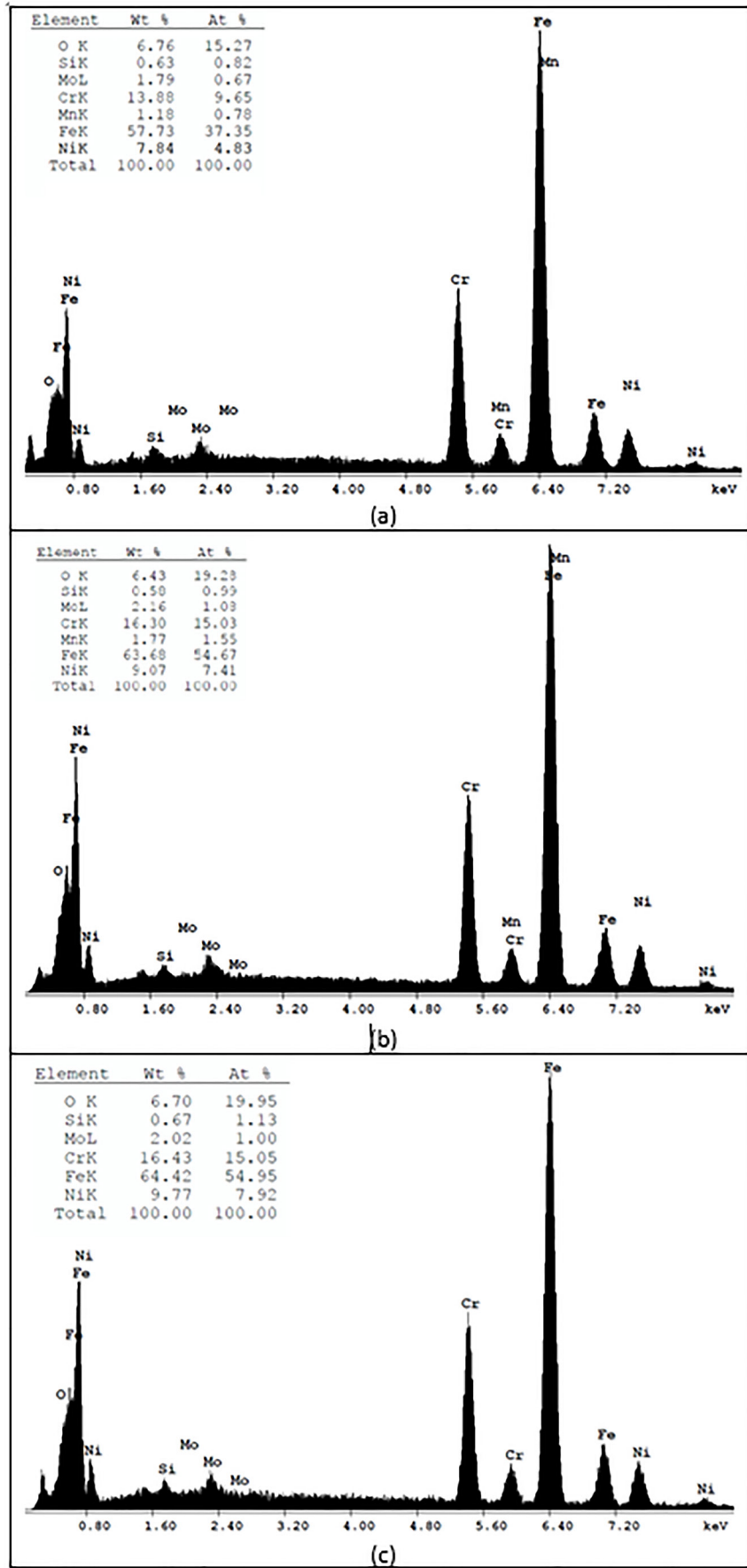


**Figure 1:** EDX analysis of the elementary chemical composition of the (a) polished 316L SS and of textured surfaces with energy densities of (b) 2.1 J/cm<sup>2</sup> and (c) 2.8 J/cm<sup>2</sup>.

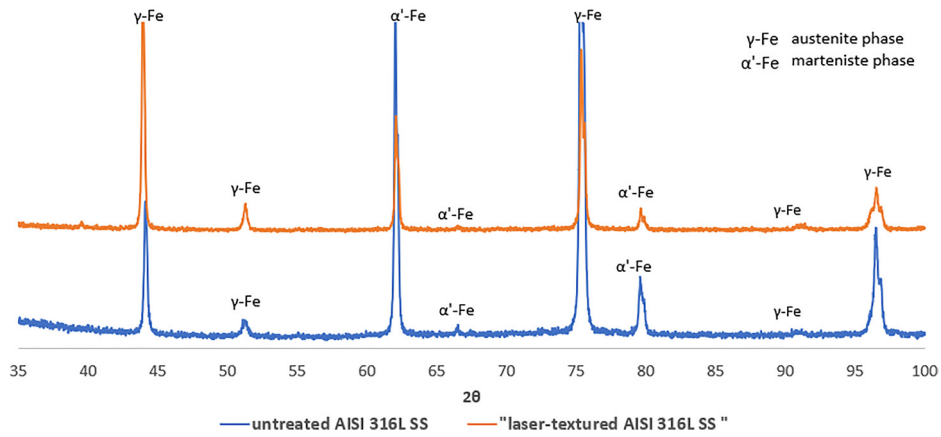


Figure 2: X-ray diffractometry results for untreated and laser-textured AISI 316L surfaces.

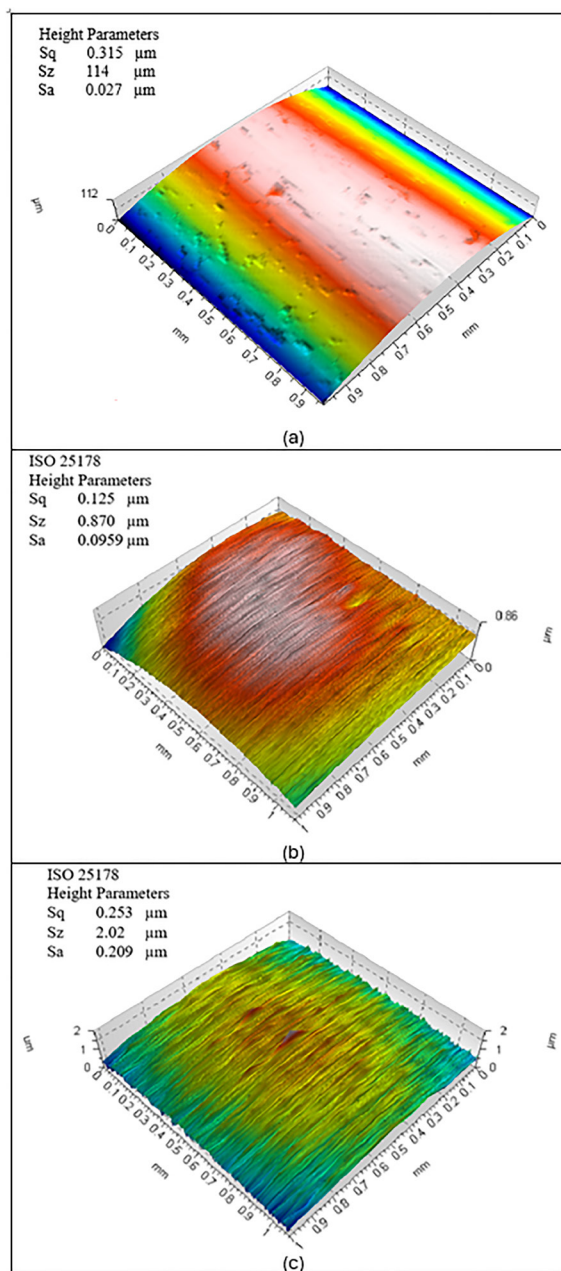
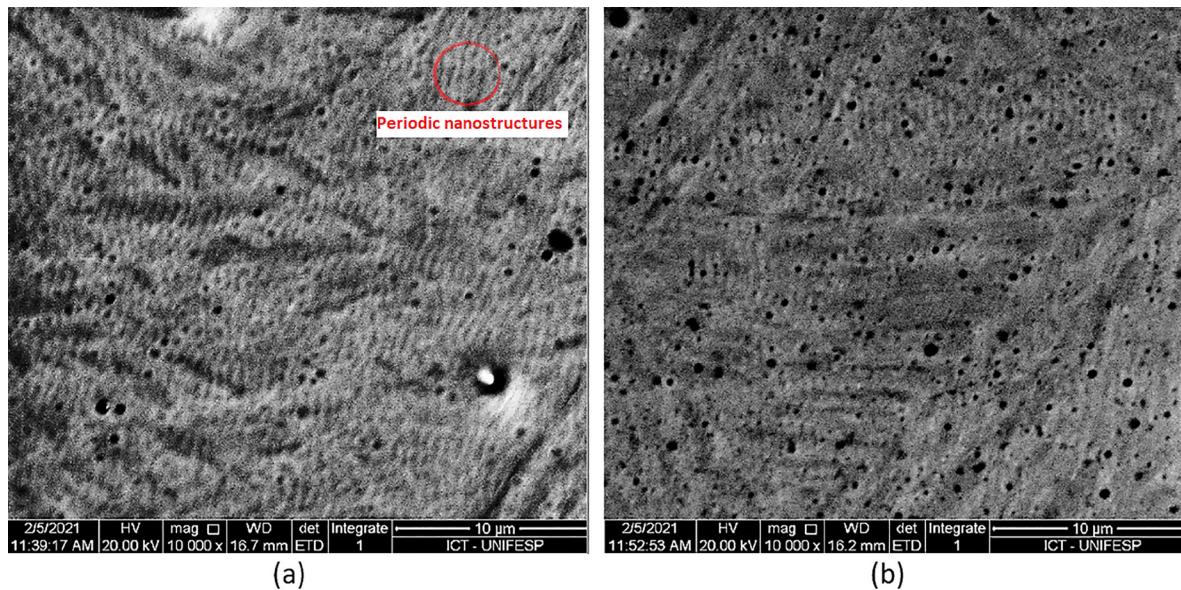


Figure 3: Topographies and roughness parameters of the (a) untreated and textured surfaces processed at (b) 2.1 J/cm<sup>2</sup> and (c) 2.8 J/cm<sup>2</sup>.



**Figure 4:** SEM images of laser-textured metal surfaces for both experimental conditions, (a) 2.1 J/cm<sup>2</sup> and (b) 2.8 J/cm<sup>2</sup>.

pulsed laser in generating these structures on steel surfaces. Previously, SIMÕES *et al.* [38] demonstrated the potential use of nanosecond pulsed lasers to generate LIPSS on the stainless steel surfaces. In this study, the authors explored the influence of irradiation parameters and surface finishing on LIPSS, concluding that surface roughness and the fluence have a significant impact on the efficient generation of LIPSS. In general, the literature reports the generation of LIPSS using femtosecond or picosecond pulsed lasers [35, 44, 45]. Although the use of these lasers presents different characteristics compared to nanosecond pulsed lasers, it has been shown that the laser fluence should fall within the range of the material melting and vaporization thresholds. EICHSTÄDT *et al.* [45] provided experimental evidence that the accumulated fluence plays a decisive role in the generation of LIPSS. Therefore, the laser fluence values considered in the present work were sufficient to generate LIPSS on AISI 316L SS, considering the control of processing parameters. It is important to highlight that in both conditions, the variations in surface roughness do not affect the generation of nanostructures, typical of LIPSS. These nanostructures remain unchanged, exhibiting a line spacing equivalent to the laser wavelength (532 nm).

### 3.2. Antibiofilm activity of the laser-textured AISI 316L SS samples

The antibiofilm properties of both untreated (control) and laser-textured surfaces were evaluated against *E. coli* and *C. albicans*. Table 2 summarizes the antimicrobial properties determined by measuring the absorbance of microorganisms deposited on the examined surfaces. An enhancement in the antimicrobial efficiency of the laser-textured surfaces (S2.1\_E and S2.8\_E) is evident, showing an increase ranging from 30% to 43% compared to the untreated surface (S\_control\_E) for the *E. coli* microorganism. Conversely, the antimicrobial effectiveness of the laser-textured surfaces is notably lower against *C. albicans*, exhibiting a marginal improvement for one of the analyzed conditions, 15% (S2.8\_C), but with a significant decrease in efficiency for another textured surface, -126% (S2.1\_C), in comparison to the untreated surface (S\_control\_C). Figure 5 provides a visual comparison of the antimicrobial efficiency values obtained for the analyzed samples.

The biofilms were visualized through Scanning Electron Microscopy (FEG-SEM). Figure 6 presents SEM images of *E. coli* with different magnifications, grown on the untreated surface (S\_control\_E, Figure 6a and 6b), and laser-textured surfaces (S2.1\_E and S2.8\_E samples), Figure 6c–d, respectively. In general, the adhesion and growth of the *E. coli* biofilm exhibit a more organized pattern with a greater number of attached cells on the untreated surface (S\_control\_E) as opposed to the laser-textured surface. Bacterial adhesion is acknowledged as the initial phase preceding biofilm development and a crucial step in pathogenesis [46]. Employing chemical or physical modifications on the material surface can inhibit bacterial adhesion and the formation of biofilm architecture, representing a strategy to improvement the surface antibacterial properties [47]. Under these conditions, the surfaces present regions without bacteria, evidencing the influence of LIPSS on the inhibition of *E. coli* biofilm growth. The bacterial cells under the influence of LIPSS demonstrated certain cell elongation and collapsed bacterial cell walls (Figure 6d and 6f). This behavior is more evident for LIPSS performed at a laser fluence of 2.1 J/cm<sup>2</sup>, which corroborates with its higher antibiofilm efficiency presented in previous results (Figure 5).

**Table 2:** Antibiofilm activity properties of the untreated and laser-textured surfaces.

SAMPLE	MICROORGANISM	ABSORBANCE	ANTIMICROBIAL EFFICIENCY (%)
S_control_E	<i>E. coli</i>	0.249	0
S2.1_E	<i>E. coli</i>	0.141	43
S2.8_E	<i>E. coli</i>	0.174	30
S_control_C	<i>C. albicans</i>	0.130	0
S2.1_C	<i>C. albicans</i>	0.294	-126
S2.8_C	<i>C. albicans</i>	0.110	15

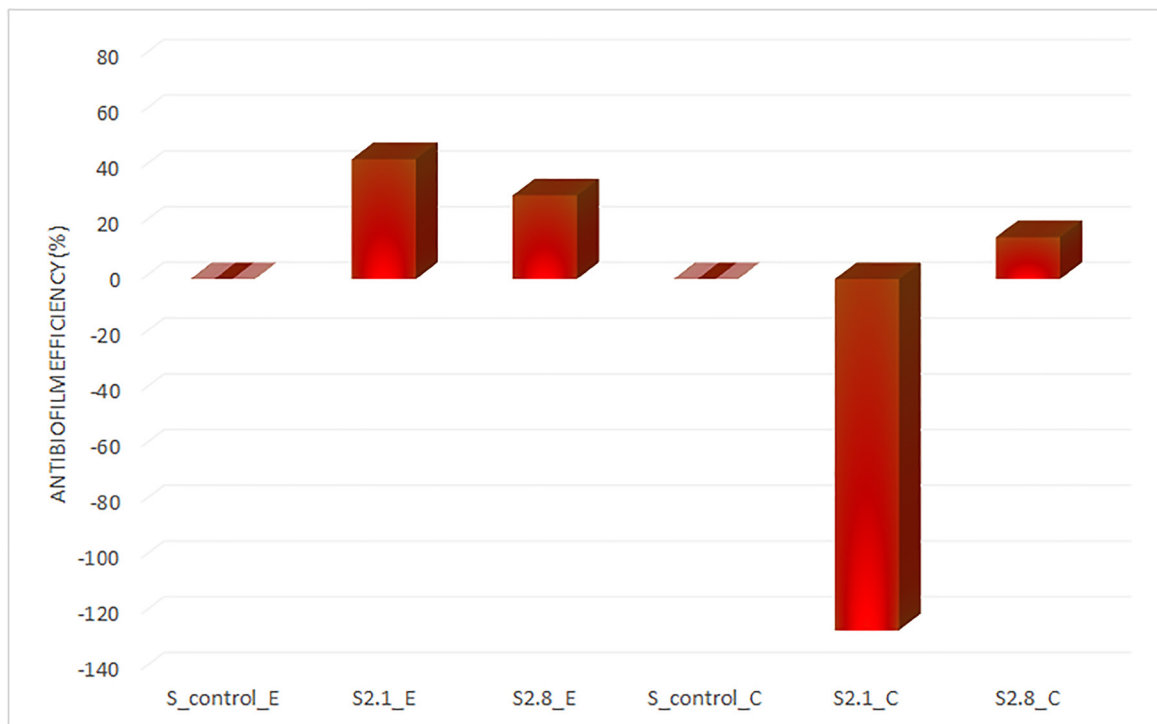
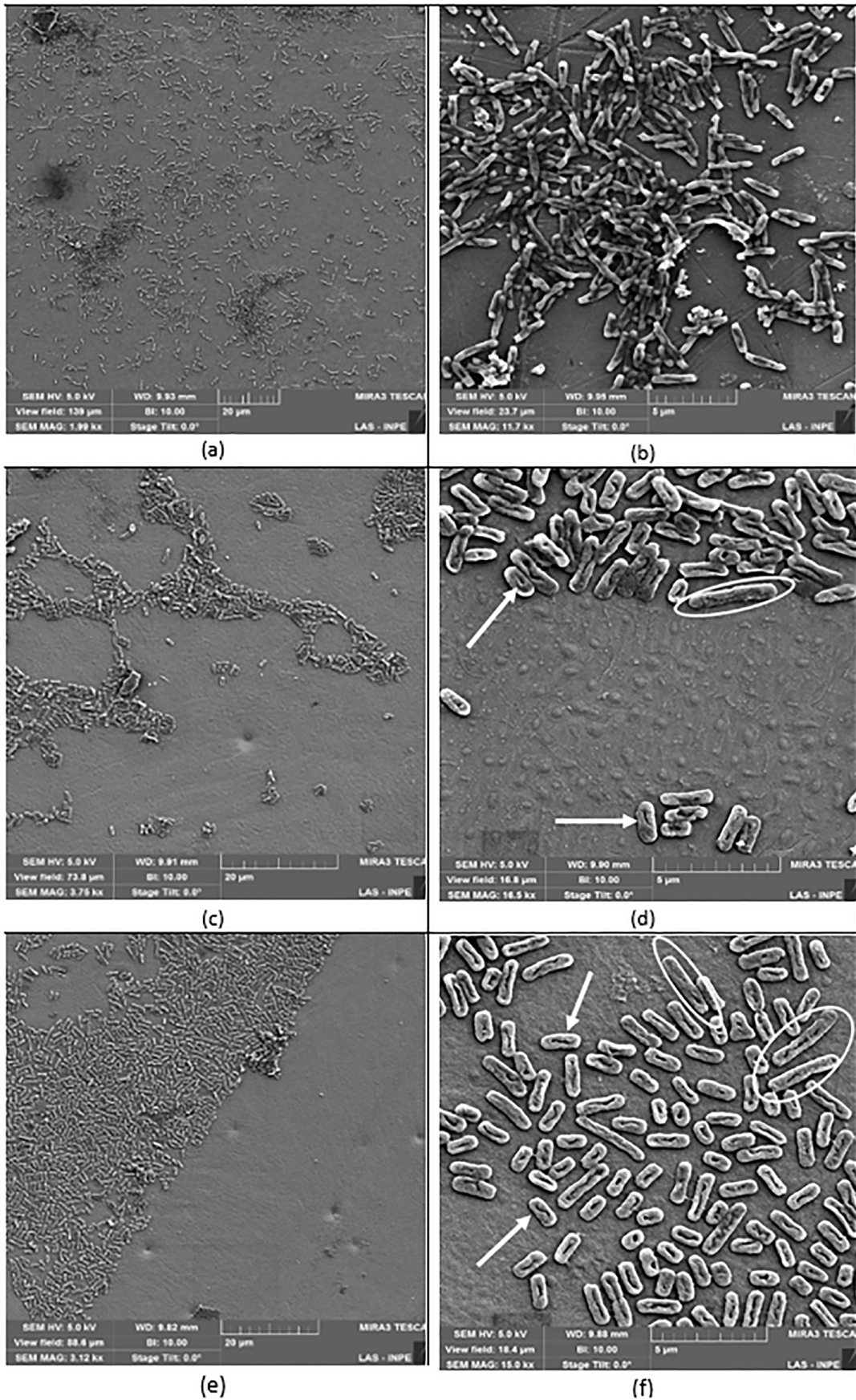
**Figure 5:** Antibiofilm efficiency of *E. coli* and *C. albicans* on the AISI 316L SS surfaces.

Figure 7 shows SEM images of *C. albicans* at low and high magnifications on the untreated surface (S\_control\_C, Figure 7a and 7b) and the laser-textured surfaces, specifically S2.1\_C and S2.8\_C samples (Figure 7c–f, respectively). A certain degree of inhibition in biofilm growth is noted on the surface textured at a fluence of 2.8 J/cm<sup>2</sup> compared to the untreated surface (control). This sample reveals the limitations in the growth and adhesion of *C. albicans* cells, accompanied by alterations in cell morphology. Alterations, consistent with findings from other study [48], encompass damage to the cell wall and membrane, pore formation, surface roughness, cell shrinkage, and few hyphae structures in the presented micrograph (Figure 7f). Biofilms of *C. albicans* with a higher hyphal content demonstrate elevated compressive strength and greater resistance to destruction. Concurrently, hyphae contribute to enhancing the organism's virulence [49]. Conversely, the surface textured with a lower fluence, 2.1 J/cm<sup>2</sup>, appeared to induce the biofilm growth after laser texturing. In the sample S2.1\_C, there is more adhered cells to the surface, as well as the presence of the beginning of EPS formation. These results align with the results obtained in the microbiological activity analysis using the CV method.

As mentioned, studies [18–24] have demonstrated that the effects of laser-textured surfaces on bacterial or fungal retention could vary. Generally, wettability and surface morphology influence a microorganism's ability to remain attached to a surface. Thereby, an increase in surface roughness tending to facilitate the adhesion and growth of a biofilm due to the larger available contact area [35, 50]. KOLLU and LAJEUNESSE [36] emphasize the importance of considering differences in responses among nanostructured surfaces when aiming to control





**Figure 6:** *E. coli* SEM images of the control (S\_control\_E, a-b) and laser-textured surfaces, (c-d) S2.1\_E and (e-f) S2.8\_E samples. Morphological changes: disruption in the outer wall and cytoplasmic membranes, and some vacuolization (arrows), and cell elongation (ellipse).

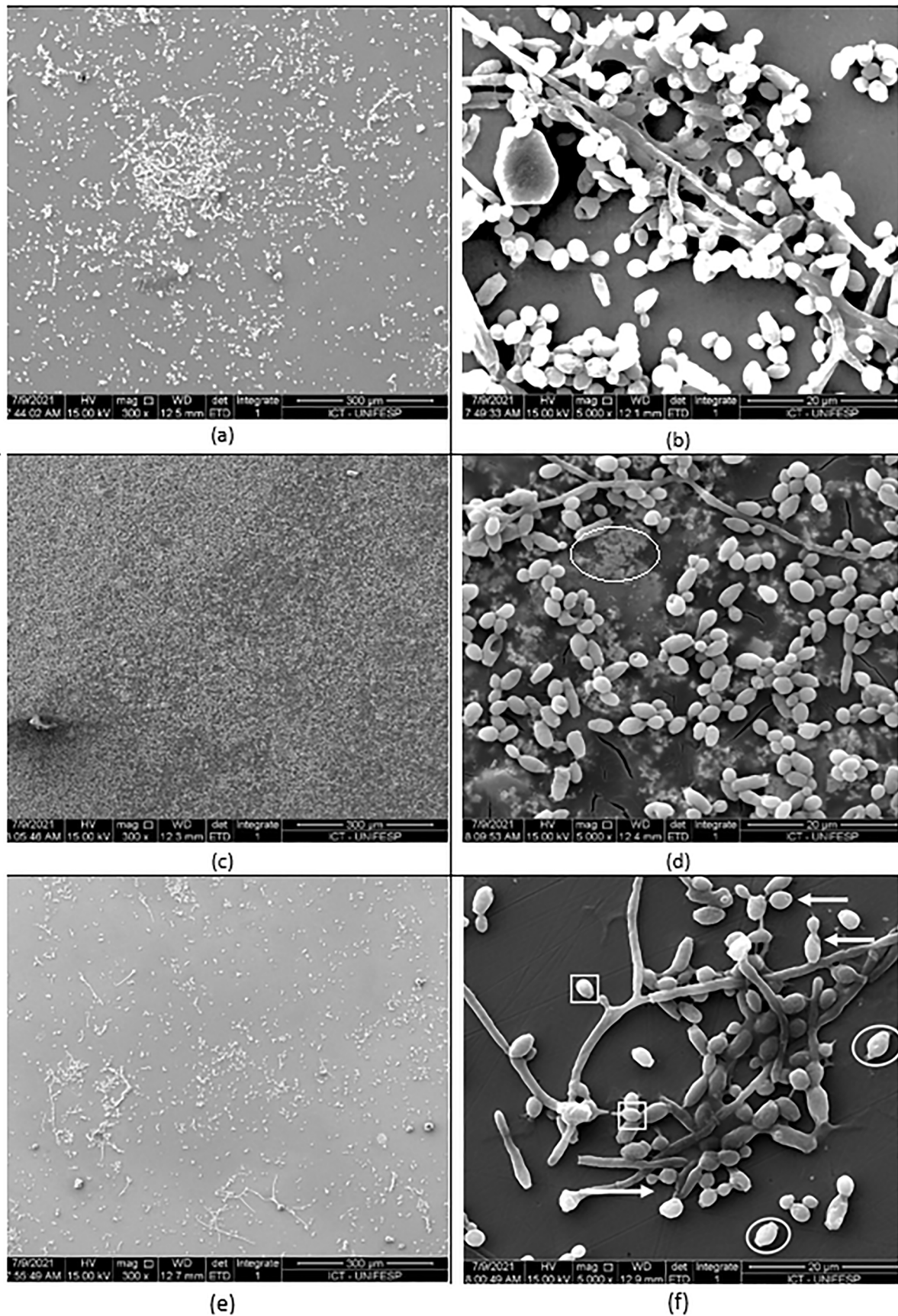


**Figure 7:** *C. albicans* SEM images of the control (S\_control\_C, a-b) and laser-textured surfaces, (c-d) S2.1\_C and (e-f) S2.8\_C samples. EPS formation (ellipse). Morphological changes: membrane pore formation (arrows), surface roughness (circles), and cell size reduction (squares).

bacterial cells or pathogenic fungal biofilms. The authors suggest that in medically relevant situations where both fungal and bacterial entities coexist, the growth of fungal biofilms might be preferential. NGUYEN *et al.* [51] conducted extensive research on the significance of surface topography and their impacts on cell adhesion. The authors showed that at the microscale, human corneal epithelial cells can alter their alignment when the surface grooves range between 0.8–1.6  $\mu\text{m}$ . Furthermore, according to WASHBURN *et al.* [52], a critical nanoscale surface roughness of about 1.1 nm can influence the proliferation rate for osteoblasts. Thus, the behavior of microorganisms on textured surfaces is complex, exerting a strong influence on their morphology, besides adhesion and growth on a solid surface.

In the present study, it is observed that the generation of Laser-Induced Periodic Surface Structures (LIPSS) on the AISI 316L stainless steel surface exhibits higher antimicrobial efficiency against *E. coli* bacteria compared to *C. albicans* fungi. In other words, the nanoscale roughness of the LIPSS formed on metallic surfaces has inhibited the growth of *E. coli*, particularly on textured surfaces at a lower average roughness of about 96 nm, processed at laser fluence of 2.1 J/cm<sup>2</sup> (S\_2.1\_E). On the other hand, LIPSS does not appear to have the same effect on *E. coli* inhibition on the textured surface with higher average roughness, of a few hundred micrometers (laser fluence of 2.8 J/cm<sup>2</sup>, S\_2.8\_E). This behavior is even more evident in the results obtained for *C. albicans* adhesion and growth on both laser-textured surfaces, where LIPSS has a low influence on the antimicrobial efficiency of the region.

#### 4. CONCLUSIONS

The successful generation of laser-induced periodic surface structures (LIPSS) on AISI 316L stainless steel surfaces using a 100-nanosecond pulsed laser marks an advancement in surface modification techniques, evidencing antimicrobial properties of these laser-textured surfaces, with reductions in *E. coli* viability ranging from 30% to 43% compared to untreated surfaces. Based on the obtained results, the following conclusions can be drawn:

- LIPSS provided evidence of inhibited growth of *E. coli* on laser-textured surfaces, highlighting its potential use in the preventing biofilm formation, with antimicrobial efficiency ranging from 30% to 43% on laser-textured surfaces against *E. coli* bacteria when compared to untreated surfaces.
- Although the efficacy of laser-textured surfaces against *E. coli* bacteria was evidenced, the effectiveness against *C. albicans* fungi was notably lower, with marginal improvements observed at higher laser fluences, 2.8 J/cm<sup>2</sup>, and a significant decrease in efficiency observed for one textured surface at 2.1 J/cm<sup>2</sup>.
- SEM visualization of biofilms confirms inhibited growth of *E. coli* on laser-textured surfaces, indicating the potential of LIPSS in inhibiting biofilm formation. Conversely, the influence of LIPSS on *C. albicans* adhesion and growth varied, with surfaces textured at higher fluences showing some inhibition while those textured at lower fluences promoted biofilm growth.

In conclusion, our findings offer valuable insights into the potential applications of the LIPSS in antimicrobial surface design. This nuanced response underscores the complexity of microbial interactions with laser-textured surfaces and emphasizes the importance of tailored approaches in antimicrobial surface engineering.

#### 5. ACKNOWLEDGMENTS

Authors would like to acknowledge FAPESP project “LIPS in 316L stainless steel to biomedical application” (process number 2020/07880-0) for the financial support. The authors thank Laboratory of Measurements of Optical Surfaces (LMSO) of the Institute of Advanced Studies for performed profilometry analysis.

#### 6. BIBLIOGRAPHY

- [1] ASRI, R.I.M., HARUN, W.S.W., SAMYKANO, M., *et al.*, “Corrosion and surface modification on biocompatible metals: a review”, *Materials Science and Engineering C*, v. 77, pp. 1261–1274, 2017. doi: <http://doi.org/10.1016/j.msec.2017.04.102>. PubMed PMID: 28532004.
- [2] YUE, T.M., YU, J.K., MAN, H.C., “The effect of excimer laser surface treatment on pitting corrosion resistance of 316L stainless steel”, *Surface and Coatings Technology*, v. 137, n. 1, pp. 65–71, 2001. doi: [http://doi.org/10.1016/S0257-8972\(00\)01104-X](http://doi.org/10.1016/S0257-8972(00)01104-X).
- [3] MOHD YUSUF, S., CHEN, Y., BOARDMAN, R., *et al.*, “Investigation on porosity and microhardness of 316L stainless steel fabricated by selective laser melting”, *Metals*, v. 7, n. 2, pp. 64, 2017. doi: <http://doi.org/10.3390/met7020064>.

- [4] ASM INTERNATIONAL, *ASM Specialty Handbook: Stainless Steels*, Ohio, ASM, 1999.
- [5] SREY, S., JAHID, I.K., HA, S.-D., “Biofilm formation in food industries: a food safety concern”, *Food Control*, v. 31, n. 2, pp. 572–585, 2013. doi: <http://doi.org/10.1016/j.foodcont.2012.12.001>.
- [6] LINKLATER, D.P., JUODKAZIS, S., IVANOVA, E.P., “Nanofabrication of mechano-bactericidal surfaces”, *Nanoscale*, v. 9, n. 43, pp. 16564–16585, 2017. doi: <http://doi.org/10.1039/C7NR05881K>. PubMed PMID: 29082999.
- [7] ARAUJO, L.V.D., GUIMARÃES, C.R., MARQUITA, R.L.D.S., *et al.*, “Rhamnolipid and surfactin: anti-adhesion/antibiofilm and antimicrobial effects”, *Food Control*, v. 63, pp. 171–178, 2016. doi: <http://doi.org/10.1016/j.foodcont.2015.11.036>.
- [8] CICCIO, P.D., VERGARA, A., FESTINO, A.R., *et al.*, “Biofilm formation by *Staphylococcus aureus* on food contact surfaces: relationship with temperature and cell surface hydrophobicity”, *Food Control*, v. 50, pp. 930–936, 2015. doi: <http://doi.org/10.1016/j.foodcont.2014.10.048>.
- [9] TSUI, C., KONG, E.F., JABRA-RIZK, M.A., “Pathogenesis of *Candida albicans* biofilm”, *Pathogens and Disease*, v. 74, n. 4, pp. ftw018, 2016. doi: <http://doi.org/10.1093/femspd/ftw018>. PubMed PMID: 26960943.
- [10] HALL-STOODLEY, L., COSTERTON, J.W., STOODLEY, P., “Bacterial biofilms: from the natural environment to infectious diseases”, *Nature Reviews. Microbiology*, v. 2, n. 2, pp. 95–108, 2004. doi: <http://doi.org/10.1038/nrmicro821>. PubMed PMID: 15040259.
- [11] NAIK, K., KOWSHIK, M., “Anti-biofilm efficacy of low temperature processed AgCl-TiO<sub>2</sub> nanocomposite coating”, *Materials Science and Engineering C*, v. 34, pp. 62–68, 2014. doi: <http://doi.org/10.1016/j.msec.2013.10.008>. PubMed PMID: 24268234.
- [12] NOBILE, C.J., JOHNSON, A.D., “*Candida albicans* biofilms and human disease”, *Annual Review of Microbiology*, v. 69, n. 1, pp. 71–92, 2015. doi: <http://doi.org/10.1146/annurev-micro-091014-104330>. PubMed PMID: 26488273.
- [13] DUFOUR, D., LEUNG, V., LEVESQUE, C.M., “Bacterial biofilm: structure, function, and antimicrobial resistance”, *Endodontic Topics*, v. 22, n. 1, pp. 2–16, 2012. doi: <http://doi.org/10.1111/j.1601-1546.2012.00277.x>.
- [14] GILLETT, A., WAUGH, D., LAWRENCE, J., *et al.*, “Laser surface modification for the prevention of biofouling by infection causing *Escherichia Coli*”, *Journal of Laser Applications*, v. 28, n. 2, pp. 022503, 2016. doi: <http://doi.org/10.2351/1.4944442>.
- [15] MANIVASAGAM, V.K., PERUMAL, G., ARORA, H.S., POPAT, K.C., “Enhanced antibacterial properties on superhydrophobic micro-nano structured titanium surface”, *J Biomed Mater Res.*, v. 110, n. 7, pp. 1314–1328, 2022. doi:10.1002/jbm.a.37375.
- [16] CAMPOCCIA, D., MONTANARO, L., ARCIOLA, C.R., “A review of the biomaterials technologies for infection-resistant surfaces”, *Biomaterials*, v. 34, n. 34, pp. 8533–8554, 2013. doi: <http://doi.org/10.1016/j.biomaterials.2013.07.089>. PubMed PMID: 23953781.
- [17] HARRIS, L.G., GEOFF, R., “*Staphylococci* and implant surfaces: a review”, *Injury*, v. 37, n. 2, pp. 3–14, 2006. doi: <http://doi.org/10.1016/j.injury.2006.04.003>. PubMed PMID: 16651069.
- [18] HSU, L.C., FANG, J., BORCA-TASCIUC, D.A., *et al.*, “Effect of micro- and nanoscale topography on the adhesion of bacterial cells to solid surfaces”, *Applied and Environmental Microbiology*, v. 79, n. 8, pp. 2703–2712, 2013. doi: <http://doi.org/10.1128/AEM.03436-12>. PubMed PMID: 23416997.
- [19] DONLAN, R.M., “Biofilm formation: a clinically relevant microbiological process”, *Clinical Infectious Diseases*, v. 33, n. 8, pp. 1387–1392, 2001. doi: <http://doi.org/10.1086/322972>. PubMed PMID: 11565080.
- [20] WOODLING, S.E., MORARU, C.I., “Influence of surface topography on the effectiveness of pulsed light treatment for the inactivation of *Listeria innocua* on stainless-steel surfaces”, *Journal of Food Science*, v. 70, n. 7, pp. m345–m351, 2005. doi: <http://doi.org/10.1111/j.1365-2621.2005.tb11478.x>.
- [21] FLINT, S.H.H., BROOKS, J.D.D., BREMER, P.J.J., “Properties of the stainless steel substrate, influencing the adhesion of thermo-resistant streptococci”, *Journal of Food Engineering*, v. 43, n. 4, pp. 235–242, 2000. doi: [http://doi.org/10.1016/S0260-8774\(99\)00157-0](http://doi.org/10.1016/S0260-8774(99)00157-0).
- [22] VERRAN, J., ROWE, D.L., BOYD, R.D., “The effect of nanometer dimension morphological features on the hygienic status of stainless steel”, *Journal of Food Protection*, v. 64, n. 8, pp. 1183–1187, 2001. doi: <http://doi.org/10.4315/0362-028X-64.8.1183>. PubMed PMID: 11510657.

- [23] WHITEHEAD, K.A., COLLIGON, J., VERRAN, J., “Retention of microbial cells in substratum surface features of micrometer and sub-micrometer dimensions”, *Colloids and Surfaces. B, Biointerfaces*, v. 41, n. 2-3, pp. 129–138, 2005. doi: <http://doi.org/10.1016/j.colsurfb.2004.11.010>. PubMed PMID: 15737538.
- [24] BOYD, R.D., VERRAN, J., JONES, M.V., *et al.*, “Use of the atomic force microscope to determine the effect of substratum surface topography on bacterial adhesion”, *Langmuir*, v. 18, n. 6, pp. 2343–2346, 2002. doi: <http://doi.org/10.1021/la011142p>.
- [25] BALASUNDARAM, G., WEBSTER, T.J., “A perspective on nanophase materials for orthopedic implant applications”, *Journal of Materials Chemistry*, v. 16, n. 38, pp. 3737–3745, 2006. doi: <http://doi.org/10.1039/b604966b>.
- [26] NIKKHAH, M., EDALAT, F., MANOUCHERI, S., *et al.*, “Engineering microscale topographies to control the cell-substrate interface”, *Biomaterials*, v. 33, n. 21, pp. 5230–5246, 2012. doi: <http://doi.org/10.1016/j.biomaterials.2012.03.079>. PubMed PMID: 22521491.
- [27] NGUYEN, A.T., SATHE, S.R., YIM, E.K., “From nano to micro: topographical scale and its impact on cell adhesion, morphology and contact guidance”, *Journal of Physics Condensed Matter*, v. 28, n. 18, pp. 183001, 2016. doi: <http://doi.org/10.1088/0953-8984/28/18/183001>. PubMed PMID: 27066850.
- [28] RAZI, S., VARLAMOVA, O., REIF, J., *et al.*, “Birth of periodic Micro/Nano structures on 316L stainless steel surface following femtosecond laser irradiation, single and multi scanning study”, *Optics & Laser Technology*, v. 104, pp. 8–16, 2018. doi: <http://doi.org/10.1016/j.optlastec.2018.02.001>.
- [29] VALETTE, S., STEYER, P., RICHARD, L., *et al.*, “Influence of femtosecond laser marking on the corrosion resistance of stainless steels”, *Applied Surface Science*, v. 252, n. 13, pp. 4696–4701, 2006. doi: <http://doi.org/10.1016/j.apsusc.2005.07.161>.
- [30] BIRNBAUM, M., “Semiconductor surface damage produced by Ruby Lasers”, *Journal of Applied Physics*, v. 36, n. 11, pp. 3688–3689, 1965. doi: <http://doi.org/10.1063/1.1703071>.
- [31] WANG, G., MOYA, S., LU, Z.F., *et al.*, “Enhancing orthopedic implant bioactivity: refining the nanotopography”, *Nanomedicine (London)*, v. 10, n. 8, pp. 1327–1341, 2015. doi: <http://doi.org/10.2217/nmm.14.216>.
- [32] BONSE, J., HÖHM, S., KIRNER, S.V., *et al.*, “Laser-induced periodic surface structures— a scientific evergreen”, *IEEE Journal of Selected Topics in Quantum Electronics*, v. 23, n. 9000615, 2017. doi: <http://doi.org/10.1109/JSTQE.2016.2614183>.
- [33] SINGH, A.K., KUMAR, B.S., JHA, P., *et al.*, “Surface micro-structuring of type 304 stainless steel by femtosecond pulsed laser: Effect on surface wettability and corrosion resistance”, *Applied Physics. A, Materials Science & Processing*, v. 124, n. 12, pp. 1–9, 2018. doi: <http://doi.org/10.1007/s00339-018-2243-8>.
- [34] MARTÍNEZ-CALDERON, M., RODRÍGUEZ, A., DIAS-PONTE, A., *et al.*, “Femtosecond laser fabrication of highly hydrophobic stainless steel surface with hierarchical structures fabricated by combining ordered microstructures and LIPSS”, *Applied Surface Science*, v. 374, pp. 81–89, 2016. doi: <http://doi.org/10.1016/j.apsusc.2015.09.261>.
- [35] LUTEY, A.H., GEMINI, L., ROMOLI, L., *et al.*, “Towards laser-textured antibacterial surfaces”, *Scientific Reports*, v. 8, n. 1, pp. 10112, 2018. doi: <http://doi.org/10.1038/s41598-018-28454-2>. PubMed PMID: 29973628.
- [36] KOLLU, N.V., LAJEUNESSE, D.R., “Cell rupture and morphogenesis control of the dimorphic yeast candida albicans by nanostructured surfaces”, *ACS Omega*, v. 6, n. 2, pp. 1361–1369, 2021. doi: <http://doi.org/10.1021/acsomega.0c04980>. PubMed PMID: 33490795.
- [37] EPPERLEIN, N., MENZEL, F., SCHWIBBERT, K., *et al.*, “Influence of femtosecond laser produced nanostructures on biofilm growth on steel”, *Applied Surface Science*, v. 418, pp. 420–424, 2017. doi: <http://doi.org/10.1016/j.apsusc.2017.02.174>.
- [38] SIMÕES, J.G.A.B., RIVA, R., MIYAKAWA, W., “High-speed Laser-Induced Periodic Surface Structures (LIPSS) generation on stainless steel surface using a nanosecond pulsed laser”, *Surface and Coatings Technology*, v. 344, pp. 423–432, 2018. doi: <http://doi.org/10.1016/j.surfcoat.2018.03.052>.
- [39] GODOY, G.G.S.M., DE ANDRADE, V.M., DONDEO, F., *et al.*, “Effect of laser thermochemical treatment of Ti-6Al-4V alloy on Candida albicans biofilm growth”, *Materials Chemistry and Physics*, v. 294, pp. 127055, 2023. <http://doi.org/10.1016/j.matchemphys.2022.127055>.

- [40] PETRACHI, T., RESCA, E., PICCINNO, M.S., *et al.*, “An alternative approach to investigate biofilm in medical devices: a feasibility study”, *International Journal of Environmental Research and Public Health*, v. 14, n. 12, pp. 1587, 2017. doi: <http://doi.org/10.3390/ijerph14121587>. PubMed PMID: 29258219.
- [41] SOHRABI, M.J., MIRZADEH, H., DEGHANIAN, C., “Significance of martensite reversion and austenite stability to the mechanical properties and transformation-induced plasticity effect of austenitic stainless steels”, *Journal of Materials Engineering and Performance*, v. 29, n. 5, pp. 3233–3242, 2020. doi: <http://doi.org/10.1007/s11665-020-04798-7>.
- [42] KRULL, R., WUCHERPFENNIG, T., ESFANDABADI, M.E., *et al.*, “Characterization and control of fungal morphology for improved production performance in biotechnology”, *Journal of Biotechnology*, v. 163, n. 2, pp. 112–123, 2013. doi: <http://doi.org/10.1016/j.jbiotec.2012.06.024>. PubMed PMID: 22771505.
- [43] BRAEM, A., VAN MELLAERT, L., MATTHEYS, T., *et al.*, “Staphylococcal biofilm growth on smooth and porous titanium coatings for biomedical applications”, *Journal of Biomedical Materials Research. Part A*, v. 102, n. 1, pp. 215–224, 2014. doi: <http://doi.org/10.1002/jbm.a.34688>. PubMed PMID: 23661274.
- [44] WU, B., ZHOU, M., LI, J., *et al.*, “Superhydrophobic surfaces fabricated by microstructuring of stainless steel using a femtosecond laser”, *Applied Surface Science*, v. 256, n. 1, pp. 61–66, 2009. doi: <http://doi.org/10.1016/j.apsusc.2009.07.061>.
- [45] EICHSTÄDT, J., RÖMER, G.R.B.E., HUIS IN ‘T VELD, A.J., “Determination of irradiation parameters for laser-induced periodic surface structures”, *Applied Surface Science*, v. 264, pp. 79–87, 2013. doi: <http://doi.org/10.1016/j.apsusc.2012.09.120>.
- [46] GHILINI, F., PISSINIS, D.E., MIÑÁN, A., *et al.*, “How functionalized surfaces can inhibit bacterial adhesion and viability”, *ACS Biomaterials Science & Engineering*, v. 5, n. 10, pp. 4920–4936, 2019. doi: <http://doi.org/10.1021/acsbiomaterials.9b00849>. PubMed PMID: 33455240.
- [47] GU, H., REN, D., “Materials and surface engineering to control bacterial adhesion and biofilm formation: a review of recent advances”, *Frontiers of Chemical Science and Engineering*, v. 8, n. 1, pp. 20–33, 2014. doi: <http://doi.org/10.1007/s11705-014-1412-3>.
- [48] WANG, J., AN, Y., LIANG, H., *et al.*, “The effect of different titanium nitride coatings on the adhesion of *Candida albicans* to titanium”, *Archives of Oral Biology*, v. 58, n. 10, pp. 1293–1301, Oct. 2013. doi: <http://doi.org/10.1016/j.archoralbio.2013.07.012>. PubMed PMID: 24011304.
- [49] EKATERINA, P., BASTIAAN P. KROM, HENNY C. VAN DER MEI, HENK J. BUSSCHER, PRASHANT K. SHARMA. Hyphal content determines the compression strength of *Candida albicans* biofilms. *Microbiology* 155(6), p. 1997–2003, 2009. <https://doi.org/10.1099/mic.0.021568-0>
- [50] PARAMONOVA, E., KROM, B.P., VAN DER MEI, H.C., *et al.*, “Hyphal content determines the compression strength of *Candida albicans* biofilms”, *Microbiology (Reading, England)*, v. 155, n. 6, pp. 1997–2003, 2009. doi: <http://doi.org/10.1099/mic.0.021568-0>. PubMed PMID: 19359323.
- [51] NGUYEN, A.T., SATHEAND, S.R., YIM, E.K.F., “From nano to micro: morphological scale and its impact on cell adhesion, morphology and contact guidance”, *Journal of Physics Condensed Matter*, v. 2, n. 18, pp. 183001, 2016. doi: <http://doi.org/10.1088/0953-8984/28/18/183001>.
- [52] WASHBURN, N.R., YAMADA, K.M., SIMON JUNIOR, C.G., *et al.*, “High-throughput investigation of osteoblast response to polymer crystallinity: influence of nanometer-scale roughness on proliferation”, *Biomaterials*, v. 25, n. 7–8, pp. 1215–1224, 2004. doi: <http://doi.org/10.1016/j.biomaterials.2003.08.043>. PubMed PMID: 14643595.